SOUTHERN PLAINS
TRANSPORTATION CENTER

MITIGATING DRY SHRINKAGE PAVEMENT CRACKING BY GEOCELL

Xiaoming Yang, Ph.D., P.E.

SPTC15.1-06-F

Southern Plains Transportation Center
201 Stephenson Parkway, Suite 4200
The University of Oklahoma
Norman, Oklahoma 73019

DISCLAIMER

The contents of this report reflect the views of the authors, who are responsible for the facts and accuracy of the information presented herein. This document is disseminated under the sponsorship of the Department of Transportation University Transportation Centers Program, in the interest of information exchange. The U.S. Government assumes no liability for the contents or use thereof.

TECHNICAL REPORT DOCUMENTATION PAGE

1. REPORT NO.	2. GOVERNMENT ACCESSION NO.	3. RECIPIENTS CATALOG NO.
SPTC15.1-06		

4. TITLE AND SUBTITLE	5. REPORT DATE
MITIGATING DRY SHRINKAGE PAVEMENT CRACKING BY GEOCELL	November 30, 2019
	6. PERFORMING ORGANIZATION CODE

7. AUTHOR(S)	8. PERFORMING ORGANIZATION REPORT
Xiaoming Yang, Ph.D., P.E.	

9. PERFORMING ORGANIZATION NAME AND ADDRESS	10. WORK UNIT NO.
School of Civil and Environmental Engineering Oklahoma State University Stillwater, Oklahoma 74078	11. CONTRACT OR GRANT NO. DTRT13-G-UTC36

12. SPONSORING AGENCY NAME AND ADDRESS	13. TYPE OF REPORT AND PERIOD COVERED
Southern Plains Transportation Center 201 Stephenson Pkwy, Suite 4200 The University of Oklahoma Norman, OK 73019	Final March 2016 – November 2019
	14. SPONSORING AGENCY CODE

15. SUPPLEMENTARY NOTES

University Transportation Center

16. ABSTRACT

Dry shrinkage cracking in pavements is currently one of the most outstanding Geotechnical problems in Oklahoma as well as in other southern plain states such as Texas and Louisiana due to the wide distribution of expansive soils in this region. The shrinkage problem on thinly pavement asphalt pavements over subgrade soil can potentially be mitigated by the use of a geocell-reinforced aggregate base layer or a geocell-reinforced soil base layer under the asphalt surface course. In this study, two types of pavement structure were recommended, asphalt concrete over a geocell reinforced aggregate base and asphalt concrete over soil base. Currently there is no design method available for flexible pavements with a geocell reinforced base. A preliminary design method was developed in this study, which is compatible to the current AASHTO MEPDG.

17. KEY WORDS	18. DISTRIBUTION STATEMENT
Geocell, geosynthetic, flexible pavement	No restrictions. This publication is available at www.sptc.org and from the NTIS.

19. SECURITY CLASSIF. (OF THIS REPORT)	20. SECURITY CLASSIF. (OF THIS PAGE)	21. NO. OF PAGES	22. PRICE
Unclassified	Unclassified	23 + cover	

SI* (MODERN METRIC) CONVERSION FACTORS

APPROXIMATE CONVERSIONS TO SI UNITS

SYMBOL	WHEN YOU KNOW	MULTIPLY BY	TO FIND	SYMBOL
		LENGTH		
in	inches	25.4	millimeters	mm
ft	feet	0.305	meters	m
yd	yards	0.914	meters	m
mi	miles	1.61	kilometers	km
		AREA		
in^2	square inches	645.2	square millimeters	mm^2
ft^2	square feet	0.093	square meters	m^2
yd^2	square yard	0.836	square meters	m^2
ac	acres	0.405	hectares	ha
mi^2	square miles	2.59	square kilometers	km^2
		VOLUME		
fl oz	fluid ounces	29.57	milliliters	mL
gal	gallons	3.785	liters	L
ft^3	cubic feet	0.028	cubic meters	m^3
yd^3	cubic yards	0.765	cubic meters	m^3
	NOTE: volumes greater than 1000 L shall be shown in m^3			
		MASS		
oz	ounces	28.35	grams	g
lb	pounds	0.454	kilograms	kg
T	short tons (2000 lb)	0.907	megagrams (or "metric ton")	Mg (or "t")
		TEMPERATURE (exact degrees)		
^oF	Fahrenheit	5 (F-32)/9 or (F-32)/1.8	Celsius	^oC
		ILLUMINATION		
fc	foot-candles	10.76	lux	lx
fl	foot-Lamberts	3.426	$candela/m^2$	cd/m^2
		FORCE and PRESSURE or STRESS		
lbf	poundforce	4.45	newtons	N
lbf/in^2	poundforce per square inch	6.89	kilopascals	kPa

APPROXIMATE CONVERSIONS FROM SI UNITS

SYMBOL	WHEN YOU KNOW	MULTIPLY BY	TO FIND	SYMBOL
		LENGTH		
mm	millimeters	0.039	inches	in
m	meters	3.28	feet	ft
m	meters	1.09	yards	yd
km	kilometers	0.621	miles	mi
		AREA		
mm^2	square millimeters	0.0016	square inches	in^2
m^2	square meters	10.764	square feet	ft^2
m^2	square meters	1.195	square yards	yd^2
ha	hectares	2.47	acres	ac
km^2	square kilometers	0.386	square miles	mi^2
		VOLUME		
mL	milliliters	0.034	fluid ounces	fl oz
L	liters	0.264	gallons	gal
m^3	cubic meters	35.314	cubic feet	ft^3
m^3	cubic meters	1.307	cubic yards	yd^3
		MASS		
g	grams	0.035	ounces	oz
kg	kilograms	2.202	pounds	lb
Mg (or "t")	megagrams (or "metric ton")	1.103	short tons (2000 lb)	T
		TEMPERATURE (exact degrees)		
^oC	Celsius	1.8C+32	Fahrenheit	^oF
		ILLUMINATION		
lx	lux	0.0929	foot-candles	fc
cd/m^2	$candela/m^2$	0.2919	foot-Lamberts	fl
		FORCE and PRESSURE or STRESS		
N	newtons	0.225	poundforce	lbf
kPa	kilopascals	0.145	poundforce per square inch	lbf/in^2

*SI is the symbol for the International System of Units. Appropriate rounding should be made to comply with Section 4 of ASTM E380.
(Revised March 2003)

MITIGATING DRY SHRINKAGE PAVEMENT CRACKING BY GEOCELL

Final Report

November 2019

Xiaoming Yang, Ph.D., P.E.

Oklahoma State University

SPTC 15.1-06

Southern Plain Transportation Center

201 Stephenson Pkwy, Suite 4200

The University of Oklahoma

Norman, Oklahoma 73019

Table of Contents

List of Figures

1. Introduction

Expansive soils are clayey soils with a large portion of Montmorillonite type minerals. Due to seasonal fluctuations of moisture content, expansive soils exhibit significant changes in volume (shrinkage and swelling). If a pavement is constructed directly on top of an expansive subgrade, shrinkage cracks in the subgrade soil developed in a dry season may propagate onto the pavement surface, which eventually forms large longitudinal cracks close to the outer edge of the pavement.

Dry shrinkage cracking in pavements is currently one of the most outstanding Geotechnical problems in Oklahoma as well as in other southern plain states such as Texas and Louisiana due to the wide distribution of expansive soils in this region (Dessouky et al. 2012). Both flexible and rigid pavement may be affected. In some cases, dry shrinkage cracks develop on a newly constructed pavement surface even before the traffic open.

Many attempts have been made in the past to mitigate the dry shrinkage cracking problem in pavements. The proposed solutions include chemical treatment (with lime or cement) (Scullion et al. 2000), geogrid-reinforcement (Zornberg, et al. 2008), moisture control products (Zhang and Presler 2012), as well as combinations of these methods (Luo and Prozzi 2009). All these methods have their limitations. Chemical treatment of soil only improve the soil properties of the top 9” to 15” of the subgrade, which does not change the shrink/swell nature of the soil underneath. Chemical treatment may also introduce additional shrinkage due to the hydration process of the stabilizer (Gaspard 2000). Geogrid-reinforcement increases the tensile strength of soil, but it requires a good interlocking with the treated soil for the tensile strength to be mobilized. Moisture control products such as drainage-capable geotextile controls the moisture of soil better when the environment is on the “wet” side than on the “dry” side, which limited its effectiveness on dry shrinkage cracking control.

Geocell is a three-dimensional geosynthetic product typically made from high density polyethylene (HDPE). It was originally developed by US Army Corps of Engineers (USACE) as a quick soil reinforcement technique (Webster 1979a and 1979b) for unpaved road constructions. Due to its three-dimensional cellular structure, geocell provides confinement to the in-fill soil without relying on particle interlocking (as in the case of geogrids). Thus, marginal geo-materials and even fine-grained soils can be stabilized (Figure 1.1). Today, geocells have been increasingly used in unpaved roads, retaining walls, railway foundation support, and erosion control projects. In a recent canal rehabilitation project in Colorado,

geocell has also been successfully used for dry shrinkage cracking control of the concrete liner (PRESTO 2014). However, most of the applications and previous research on geocell focused on the effect of improving strength and stiffness of soil (Yang and Han 2013, Yang et al. 2013). No literature was found on applications of geocell in dry shrinkage cracking control for pavements.

Figure 1.1 Geocell-confined soil (picture from prestogeo.com)

The objective of this research is to explore the feasibility of using geocell-reinforced pavement to mitigate the shrinkage problems and to develop a preliminary design method. Two types of potential pavement structures were considered: (1) asphalt concrete over geocell-reinforced aggregate base and (2) asphalt concrete over geocell-reinforced soil base.

2. Literature Review

In late 1970s, U.S. Army Engineer Waterways Experiment Station performed a series of research studies (Webster and Watkins 1977; Webster 1979a; Webster 1979b) to develop rapid and effective soil reinforcement techniques. Such techniques would help build roads quickly on unstable soils to support military vehicles. Webster and Watkins (1977) built seven unpaved test road sections (one unreinforced control section and six sections with different types of reinforced base course) on soft clay to compare different reinforcement techniques. By measuring the rut depth developed on the road after traffic loading, they found that one of the sections with a 12 inch thick sand (not a suitable material for base course) base course reinforced by cellular-confinement (made up of isolated plastic tubes of 6 inch diameter and 1 foot long) marginally outperformed the control section with a 14 inch thick crushed stone base course. After this study, a cellular confinement system, named "grid cell", was soon developed, which is made up of square shaped grids and filled with sand. To assist design and application, both laboratory model test (Rea and Mitchell 1978) and full-scale road test (Webster 1979a; Webster 1979b) were performed to investigate a variety of factors that may influence the behavior of grid cell reinforced Sand. The factors evaluated in these studies include grid size, grid shape, grid material, thickness of the sand-grid layer, subgrade stiffness, type of sand, compaction, load type, etc. These test data were later summarized and analyzed by Mitchell et al. (1979), who then proposed some useful analytical formulas to predict the capacity of the grid cell reinforced sand base course against different failure modes.

The grid cell used in Webster's (1979b) test study was made of paper and aluminum. Both materials have some drawbacks since paper has a poor resistance to water and aluminum is relatively expensive. Webster (1979b) further suggested that plastic might be a good material worth investigation. In 1980s, polymeric cellular confinement product was developed, and the general term "geocell" was first used to refer to this kind of products. Meanwhile, the benefit of using geocell reinforcement was widely demonstrated and studied in the U.S. as well as in Europe and Asia. Today geocell has been successfully used as a quick and effective soil reinforcement technique in retaining wall, foundation, and pavement structures.

The use of geocell to reinforce pavement base course has been limited for two main reasons. Although geocell has been proved to be efficient in reducing the permanent deformation in pavement, very little

effort was made to develop a design method for geocell reinforcement. The recommended configuration (cell size, thickness, etc.) of geocell reinforced base provided by the test study cannot be simply apply to another situation with different soil type or different geocell product. A rational design model is needed to predict the pavement response (such as resilient modulus and permanent deformation) with consideration of geocell reinforcement.

The only design method for geocell reinforce road base was proposed by Mengelt et al. (2000), who performed laboratory resilient modulus test on unreinforced and single-geocell-reinforced soils. Both cohesive and granular soils were used as the infill material. A special chamber was made for the single-geocell-reinforced sample because the diameter of such sample (25cm) was larger than the standard diameter (15cm) of sample for the test equipment. Test results showed that the resilient modulus of geocell-reinforced granular soil was slightly (1.4% to 3.2%) larger than that of unreinforced granular soil, whereas the resilient modulus of geocell-reinforced fine-grained soil increased 16.5% to 17.9% compared with that of the unreinforced soil. As for permanent deformation, the permanent deformation reduced by 50% for aggregate sample and 44% for sand sample when geocell reinforcement was included. Mengelt et al. (2000) also proposed a method to incorporate these findings into the flexible pavement design method (Huang 1993).

No published literature was found on numerical modeling of geocell-reinforced soil supporting repeated load. Some researcher (Perkins 2004; Kwon et al. 2009) modeled geogrid-reinforced aggregate road base based on the framework of the mechanistic-empirical model. Although the reinforcement mechanism of geogrid and geocell are quite different, these numerical models provided valuable understandings on the problem which is very helpful for this study. For example, Perkins (2004) and Kwon et al. (2009) both emphasized the importance of considering the residual horizontal stress within the base course induced by compaction. In Perkins' model, an isolated compaction model has to run first to calculate the residual stress induced by compaction. The residual stress was estimated indirectly by shrink the geocell by 1% strain horizontally. And then two traffic models (Traffic I and II) are used to calculate the residual stress in the base after a certain number of wheel passes. Finally, the residual stress obtained from traffic models is assigned as the initial stress to the response model (Traffic III) for calculating the resilient response of the pavement. Perkins (2004) also developed a permanent deformation model for geogrid reinforced soil, which must be calibrated performing cyclic triaxial test on geogrid reinforced soil samples. Kwon et al. (2009) directly assigned a 41 kPa initial horizontal stress to the base within 102mm above the geogrid to consider the compaction effect. They used an

anisotropic resilient modulus model for the aggregate base to account for the different behavior of soil under cyclic axial stress and cyclic confining stress. Due to the planar geometry of geogrid, Perkins (2004) and Kwon et al. (2009) both used two-dimensional (axisymmetric) models.

3. Development of a Preliminary Design Method

In this chapter, a preliminary design method is developed based on the current AASHTO Mechanistic-Empirical Pavement Design Guide (MEPDG). The design model for flexible pavement in the MEPDG has two important components, the response model and the damage model. The response model utilizes the layered elastic solution (by Burmister 1943, 1945) to calculate the response of the pavement at critical locations under one single wheel load. Then the damage model projects the distress (cracking, rutting, etc.) of the pavement structure based on response output from the response model. The above two-step calculation is repeated all truck load configurations and climate conditions throughout the design life of the pavement. The calculation procedure for a typical pavement design project is therefore very lengthy, thus it is not feasible to perform a hand calculation. AASHTO provided a computer program (Pavement-ME), and it is currently used by some states to run the MEPDG design.

Since the current Pavement-ME program does not allow for input of geosynthetic reinforcement. There are only two ways to consider the geocell reinforcement on the design. The first way is to change the input parameters of the reinforced material. The second way is to change the calibration factors in the damage model.

Modified Layered Elastic Solution with Reinforcement

The response of a multi-layered elastic system to a distributed load on the surface was originally calculated by Bermister (1943). This model was adopted into the MEPDG to calculate the response of a pavement structure under a single wheel load. The original version of the model cannot consider external reinforcement inside the multi-layered system. XXXX (1956) proposed a modified solution to include a thin layer of reinforcement into the interface between any of two layers in the pavement structure. The modified model introduces three additional material parameters of the reinforcement, the elastic modulus E_g, the Poisson's ratio ν_g, and the thickness of the reinforcement sheet t_g.

However, geocell is not a thin sheet type of material. The thickness of the geocell structure is the same as the reinforced layer. Therefore, in this study, it is assumed that the effect of geocell can be equivalent to three layers of 1-mm thick reinforcement sheets at the top, the middle, and the bottom of the geocell-reinforced layer. In order to obtain the equivalent plane material parameters, it is further assumed that the structure of geocell pocket is regular hexagon (honeycomb).

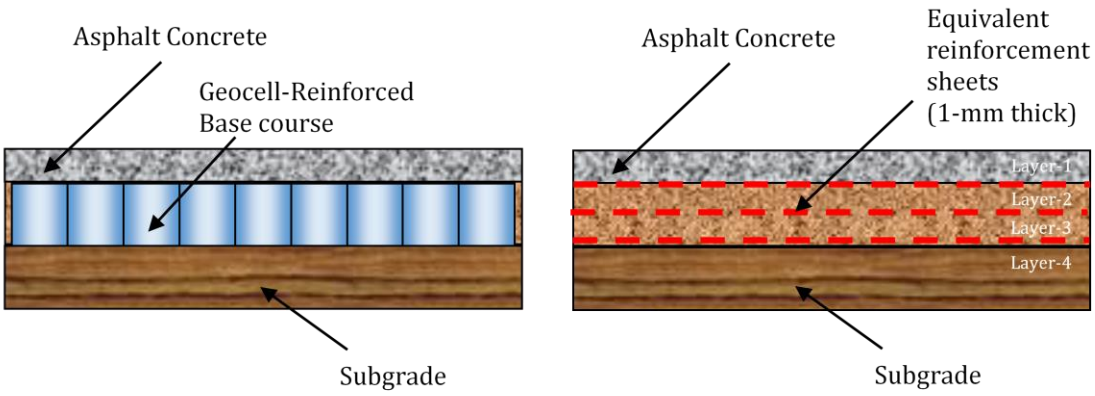

(a) Geocell reinforced pavement structure (b) Equivalent 4-layer pavement structure

Figure 3.1 Equivalency of geocell to sheet reinforcement

Based on the basic theory of cellular structure mechanics, the equivalent plain reinforcement of each of the three layers can be determined by:

$$E_g = 21\left(\frac{T}{\sqrt{L^2 + W^2}}\right)^3 \left(\frac{H}{1\text{ mm}}\right) E_s \tag{3.1}$$

$$\nu_g = 1 \tag{3.2}$$

$$t_g = 1\text{ mm} \tag{3.3}$$

where

T = thickness of the geocell sheet (without texture)

L = length of the geocell pocket

W = width of the geocell pocket

H = height of the geocell

E_s = elastic modulus of the geocell sheet

In this study, a typical three-layer pavement (with a surface course, a base course, and the subgrade) is considered. Due to the equivalency illustrated in Figure 3.1, the pavement structure in Figure 3.1a is equivalent to a four-layer system shown in Figure 3.1b. The second and the third layers are both base course material. The interface boundary condition is modified to reflect the inclusion of the geosynthetic reinforcement. A MathCAD worksheet was developed to carry out the calculation.

The calculated vertical stress at the top of the subgrade layer can be used to estimate the resilient modulus of the reinforced base course. The estimated resilient modulus, which is expected to be higher than the unreinforced base resilient modulus, can be used as an input in the MEPDG program. Due to the incensement in the base modulus, all pavement distresses calculated by the program should be reduced.

Modified Rutting Model for reinforced layer

The total rutting of a flexible pavement at any time in the design period can be calculated from the sum of the rutting from the surface course, base course, subbase course(s), and the subgrade. When a geocell reinforced base course is presented, the permanent deformation of the reinforced layer is mitigated due to the lateral confinement provided by the geocell. In this study, an analytical model is proposed to estimate the reduced permanent deformation. The analytical model considers a cylinder aggregate (or soil sample) under a repeated load triaxial (RLT) compression test.

First, consider a cylindrical sample of unreinforced unbound granular material (UGM) subjected to a constant confining stress σ_3 and a repeated deviatoric stress $\sigma_1 - \sigma_3$, assuming that the applied stress level does not exceed the shakedown limit of the material and that the sample will reach an elastic state (also called the resilient state) after a large number of load repetitions. At this stage, all the elastic strain generated in the loading period will recover in the following unloading period, and the stress-strain relationship of the sample can be described using the resilient modulus M_r.

$$\varepsilon_{1,r} = \frac{\sigma_1 - \sigma_3}{M_r} \tag{3.4}$$

where $\varepsilon_{1,r}$ = the axial resilient strain. It is well known that the resilient modulus M_r of the UGM is a stress-dependent material property. Eq. (3.5) is used to describe the stress dependency of the resilient modulus of the UGM.

$$M_r = k_1 p_a \left(\frac{\theta}{p_a}\right)^{k_2} \left(\frac{\tau_{oct}}{p_a} + 1\right)^{k_3} \tag{3.5}$$

where k_1, k_2, and k_3 = resilient modulus parameters of the material; p_a = atmosphere pressure; and θ and τ_{oct} = bulk stress and octahedral shear stress, respectively. In the triaxial test condition ($\sigma_2 = \sigma_3$), θ and τ_{oct} can be expressed as

$$\theta = \sigma_1 + \sigma_3 \tag{3.6}$$

$$\tau_{oct} = \frac{2}{3}(\sigma_1 - \sigma_3) \tag{3.7}$$

The RLT test often runs to a large number of load repetitions (e.g., 10^4 cycles). The permanent deformation behavior of the material is often characterized by the relationship between the axial permanent strain $\varepsilon_{1,p}$ (or the ratio of $\varepsilon_{1,p}$ to $\varepsilon_{1,r}$) and the number of load repetitions N. Many empirical models have been proposed to describe such a relationship. Tseng and Lytton's (1989) model [Eq. (3.8)] is selected in this study because it is the basis of the permanent deformation model for UGMs adopted in the current MEPDG.

$$\frac{\varepsilon_{1,p}}{\varepsilon_{1,r}} = \left(\frac{\varepsilon_0}{\varepsilon_r}\right) e^{-\left(\frac{\rho}{N}\right)^{\beta}} \tag{3.8}$$

where $(\varepsilon_0/\varepsilon_r)$, ρ, and β = permanent deformation parameters of the UGM, which can be determined by fitting the measured permanent deformation test curve. The form of Tseng and Lytton's (1989) model implies that the sample reaches the resilient state (the permanent deformation becomes constant) when N approaches infinity. At the resilient state, the accumulated permanent deformation approaches the value of $(\varepsilon_0/\varepsilon_r)$, . In practice, however, the value of $(\varepsilon_0/\varepsilon_r)$, , obtained from regression sometimes may be unreasonably large, especially when the shape of the measured permanent deformation curve has not approached a constant. It is therefore necessary to set a limit to the load repetition N in Eq. (5) to estimate the value of $\frac{\varepsilon_{1,p}}{\varepsilon_{1,r}}$ when the sample reaches the resilient state. For most UGMs, 10^5 load repetitions should be adequate for the sample to reach the resilient state.

Now consider a geocell-reinforced UGM cylindrical sample subjected to a constant confining stress σ_3 and a repeated deviatoric stress $\sigma_1 - \sigma_3$. When the sample reaches the resilient state, the soil has already developed some amount of permanent strain in both the axial direction ($\varepsilon_{1,p}$) and the lateral direction ($\varepsilon_{3,p}$). The lateral expansive permanent strain of the sample will induce an additional confining

stress $\Delta\sigma_3$ from the geocell to the UGM. In a geocell-reinforced sample, the additional confining stress can be assumed to be applied uniformly through the hoop stress.

Before establishing the stress-strain relationship of the reinforced sample, it should be noted that the resilient modulus M_r is defined as the secant modulus when the stress state of the soil is changed from the hydrostatic state ($\sigma_1 = \sigma_3$) to another stress state with an increased σ_1 ($\sigma_1 > \sigma_3$). Actually, it does not matter if the axial stress increases or decreases because the major and minor principal stresses are exchangeable. Therefore, the stress-strain behavior for a reinforced UGM sample in a loading cycle (the axial stress increases from σ_3 to σ_1) has to be analyzed in two consequent stages. In Stage 1, the axial stress increases from σ_3 to $\sigma_3 + \Delta\sigma_3$ so that the UGM sample reaches a hydrostatic state (i.e., confining stress = axial stress = $\sigma_3 + \Delta\sigma_3$). In Stage 2, the axial stress continues to increase from $\sigma_3 + \Delta\sigma_3$ to σ_1. The stress-strain relationships in these two stages are derived as follows:

Stage 1: The axial stress increases from σ_3 to $\sigma_3 + \Delta\sigma_3$. The resilient modulus in this stage $M_{r,1}$ can be determined by Eq. (3.5) with

$$\theta = 3\sigma_3 + 2\Delta\sigma_3 \tag{3.9a}$$

$$\tau_{oct} = \frac{\sqrt{2}}{3}\Delta\sigma_3 \tag{3.9b}$$

Stage 2: The axial stress continues to increase from $\sigma_3 + \Delta\sigma_3$ to σ_1. The resilient modulus in this stage $M_{r,2}$ can be determined by Eq. (3.5) with

$$\theta = \sigma_1 + 2(\sigma_3 + \Delta\sigma_3) \tag{3.10a}$$

$$\tau_{oct} = \frac{\sqrt{2}}{3}[\sigma_1 - (\sigma_3 + \Delta\sigma_3)] \tag{3.10b}$$

Therefore, the full resilient stress-strain relationship of the reinforced sample can be derived by combining the preceding two stages

$$\varepsilon_{1,r} = \frac{\Delta\sigma_3}{M_{r,1}} + \frac{\sigma_1 - (\sigma_3 + \Delta\sigma_3)}{M_{r,2}} = \frac{\sigma_1 - \sigma_3}{M_{r,reinf}} \tag{3.11}$$

It should be noted that the cyclic load of Stage 1 results in an axial extension, whereas the cyclic load of Stage 2 results in an axial compression. Based on Eq. (3.8), these two components together result in the overall axial permanent deformation $\varepsilon_{1,p}$ when the sample reaches the resilient state.

$$\varepsilon_{1,p} = \left[-\frac{\Delta\sigma_3}{M_{r,1}} + \frac{\sigma_1 - (\sigma_3 + \Delta\sigma_3)}{M_{r,2}}\right]\left(\frac{\varepsilon_0}{\varepsilon_r}\right) e^{-\left(\frac{\rho}{N_{limit}}\right)^{\beta}} \tag{3.12}$$

The next step is to establish the relationship between the additional confining stress $\Delta\sigma_3$ and the permanent strain of the sample. For a geocell-reinforced UGM sample, assuming that the tensile stress in the geocell is uniform along the height of the sample (i.e., the geocell deforms as a right cylinder), the hoop stress of the geocell can be calculated as

$$\Delta\sigma_3 = \frac{2M}{D}\left(\varepsilon_{1,p}\right) \tag{3.13}$$

Where M is the tensile stiffness of the geocell material and D is the equivalent pocket diameter of the geocell.

Substitute Eq. (3.12) into Eq. (13) gives

$$\Delta\sigma_3 = \frac{M}{D}\left[-\frac{\Delta\sigma_3}{M_{r,1}} + \frac{\sigma_1 - (\sigma_3 + \Delta\sigma_3)}{M_{r,2}}\right]\left(\frac{\varepsilon_0}{\varepsilon_r}\right) e^{-\left(\frac{\rho}{N_{limit}}\right)^{\beta}} \tag{3.14}$$

Eq. (3.14) can be solved by iteration. With $\Delta\sigma_3$ obtained, Eq. (3.11) can be used to calculate the resilient modulus $M_{r,reinf}$ and the resilient strain $\varepsilon_{1,r}$ of the reinforced UGM sample. Then Eq. (3.12) can be used to calculate the axial permanent deformation $\varepsilon_{1,p}$ at any load repetition N.

It should be noted that, based on the equation above, the geocell increases the resilient modulus of the base material by a constant factor k_M.

$$k_M = \left(\frac{\sigma_1 - \sigma_3}{M_r}\right) / \left[\frac{\Delta\sigma_3}{M_{r,1}} + \frac{\sigma_1 - (\sigma_3 + \Delta\sigma_3)}{M_{r,2}}\right] \tag{3.15}$$

Similarly, the permanent deformation in the reinforced base course reduced by a constant factor k_R.

$$k_R = \left[-\frac{\Delta\sigma_3}{M_{r,1}} + \frac{\sigma_1 - (\sigma_3 + \Delta\sigma_3)}{M_{r,2}}\right] / \left(\frac{\sigma_1 - \sigma_3}{M_r}\right) \tag{3.16}$$

The two factors k_M and k_R can be used in the MEPDG design for geocell-reinforced asphalt pavements. Two examples are presented in the next chapter.

4. Design Examples

This chapter presents two design example using the MEPDG. Example 1 is an asphalt pavement over geocell-reinforced aggregate base. Example 2 is an asphalt pavement over geocell-reinforced soil base. The calculation of both example was done with MathCAD spread sheets.

Example 1 Asphalt pavement over geocell-reinforced aggregate base

Design Input

Geocell (Presto GW20V):

Opening Length $L = 224\ mm$ Opening Width $W = 259\ mm$

Depth $H = 100\ mm$ Wall thickness $T = 1.3\ mm$ (Assumed)

Elastic Modulus $E_s = 200\ MPa$ (Assumed)

Tensile Stiffness: $M = E_s.T = 260\frac{kN}{m}$

Equivalent Pocket Diameter: $D = \frac{2\sqrt{L^2+W^2}}{\pi} = 218\ mm$

Equivalent 3-layer properties: $E_g = 21\left(\frac{T}{\sqrt{L^2+W^2}}\right)^3\left(\frac{H}{1\ mm}\right)E_s = 0.23\ MPa$

Base Material: $Sand$

$K_1 = 42$ $K_2 = 0.57$ $K_3 = 0$ $\varepsilon_0\varepsilon_r = 80$ $\rho = 1000$ $\beta = 0$

Stress Condition (Estimated)

$\sigma_1 = 42\ kPa$ $\sigma_3 = 14\ kPa$

Bulk Stress: $\theta = \sigma_1 + 2\sigma_3 = 70\ kPa$

Octahedral shear stress: $\tau_{oct} = \frac{\sqrt{2}}{3}(\sigma_1 - \sigma_3) = 13.2\ kPa$

Atmosphere pressure: $p_a = 101.3\ kPa$

Resilient modulus of unreinforced soil: $M_r = k_1.p_a\left(\frac{\theta}{p_a}\right)^{k_2}\left(\frac{\tau_{oct}}{p_a}+1\right)^{k_1} = 35.5\ MPa$

Step 1 -Solve $\Delta\sigma_3$ graphically by plotting both sides of Eq. 3.14.

$\Delta\sigma_3 = 0\ kPa, 2\ kPa, \ldots 12\ kPa$

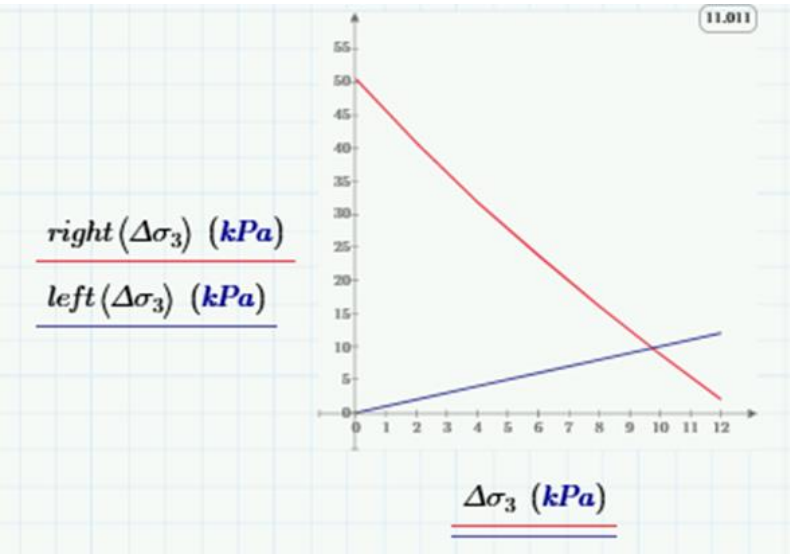

From the above graph, $\Delta\sigma_3 = 9.7\ kPa$

Step 2 – Determine the resilient modulus for the reinforced base by Eq. 3.15.

Resilient modulus improvement factor: $k_M(9.4\ kPa) = 1.062$

$$M_{r,reinf} = 1.062\ M_r = 37.7\ MPa$$

Step 3 – Determine the reduction factor k_R from Eq. 3.16.

$$k_R(9.2\ kPa) = 0.23$$

Step 4 – Use *M_r = 37.8 MPa* and *k_R = 0.23* for the reduction factor of rutting for the base course in the MEPDG design.

Example 2 Asphalt pavement over geocell-reinforced soil base

Design Input

Geocell (Presto GW20V):

Opening Length $L = 224\ mm$ Opening Width $W = 259\ mm$

Depth $H = 100\ mm$ Wall thickness $T = 1.3\ mm$ (Assumed)

Elastic Modulus $E_s = 200\ MPa$ (Assumed)

Tensile Stiffness: $M = E_s.T = 260\frac{kN}{m}$

Equivalent Pocket Diameter: $D = \frac{2\sqrt{L^2+W^2}}{\pi} = 218\ mm$

Equivalent 3-layer properties: $E_g = 21\left(\frac{T}{\sqrt{L^2+W^2}}\right)^3\left(\frac{H}{1\ mm}\right)E_s = 0.023\ MPa$

Base Material: $Soil$

$K_1 = 397$ $K_2 = 0.49$ $K_3 = 0 - 24$ $\varepsilon_0\varepsilon_r = 130$ $\rho = 2000$ $\beta = 0.4$

Stress Condition (Estimated)

$\sigma_1 = 42\ kPa$ $\sigma_3 = 14\ kPa$

Bulk Stress: $\theta = \sigma_1 + 2\sigma_3 = 70\ kPa$

Octahedral shear stress: $\tau_{oct} = \frac{\sqrt{2}}{3}(\sigma_1 - \sigma_3) = 13.2\ kPa$

Atmosphere pressure: $p_a = 101.3\ kPa$

Resilient modulus of unreinforced soil: $M_r = k_1.p_a\left(\frac{\theta}{p_a}\right)^{k_2}\left(\frac{\tau_{oct}}{p_a}+1\right)^{k_1} = 32.6\ MPa$

Step 1 -Solve $\Delta\sigma_3$ graphically by plotting both sides of Eq. 3.14.

$\Delta\sigma_3 = 0\ kPa, 2\ kPa, \ldots 12\ kPa$

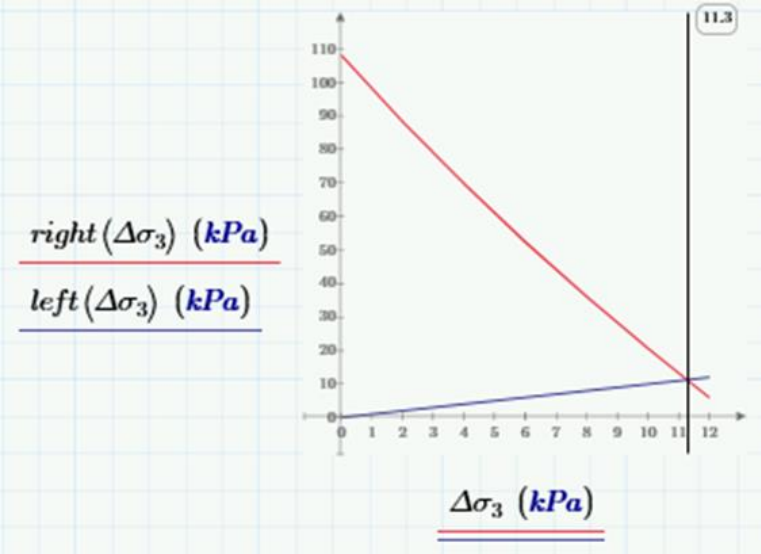

From the above graph, $\Delta\sigma_3 = 11.3\ kPa$

Step 2 – Determine the resilient modulus for the reinforced base by Eq. 3.15.

Resilient modulus improvement factor: $k_M(9.4\ kPa) = 1.079$

$$M_{r,reinf} = 1.062\ M_r = 35.2\ MPa$$

Step 3 – Determine the reduction factor k_R from Eq. 3.16.

$$k_R(9.2\ kPa) = 0.101$$

Step 4 – Use *M_r = 35.2 MPa* and *k_R = 0.101* for the reduction factor of rutting for the base course in the MEPDG design.

5. Summary and Recommendations

The shrinkage problem on thinly pavement asphalt pavements over subgrade soil can be potentially mitigated by the use of a geocell-reinforced aggregate base layer or a geocell-reinforced soil base layer under the asphalt surface course. Currently there is no design method available for flexible pavements with a geocell reinforced base. A preliminary design method was developed which is compatible to the current AASHTO MEPDG. Due to the limited time of this project, field trial section test was not conducted. It is recommended that ODOT locates a suitable project in districts with expansive soil issues to incorporate a geocell reinforced base section and then monitor the performance for a few years.

6. References

Bulut, R., Zaman, M., Amer, O., Mantri, S., Chen, L., Tian, Y., and Taghichian, A. (2009). *Drying Shrinkage Problems in High-Plastic Clay Soils in Oklahoma*. OkTC Research Report OTCREOS11.1-09-F, Oklahoma State University, Stillwater, OK.

Dessouky, S., Oh, J. H., Yang, M., Ilias, M., Lee, S. I., Freeman, T., Bourland, M., and Jao, M. (2012). *Pavement Repair Strategies for Selected Distresses in FM Roadways*. TxDOT Research Report FHWA/TX-11/0-6589-1, The University of Texas at San Antonio, San Antonio, TX.

Gaspard, K. J. (2000). Evaluation of Cement Treated Base. Technical Assistance Report Number 00-1TA, Louisiana Transportation Research Center, Baton Rouge, LA.

Luo, R., and Prozzi, J. (2009). "Combining geogrid reinforcement and lime treatment to control dry land longitudinal cracking." *Transportation Research Board, Journal of Transportation Research Record*, 2014, 88-96.

PRESTO Geosystems. (2014). *Flexible Alternative for Irrigation Canal Lining*. On line document. http://www.prestogeo.com/downloads/Bj5ygfXc3guxwnTwoGmWtw7cfj7seP3fzwUVSrxLOh0BLSxzYZ/Colorado%20Irrigation%20Canal%20Lining.pdf, accessed 9/1/2015.

Sebesta, S. and Scullion, T. (2004). *Effectiveness of Minimizing Reflective Cracking in Cement-Treated Bases by Micro-Cracking*. TxDOT Research Report FHWA/TX-05/0-4502-1. Texas Transportation Institute, College Station, TX.

Scullion, T., Sebesta, S., Harris, J. P., and Syed, I. (2000). *A Balanced Approach to Selecting the Optimal Cement Content for Soil-Cement Bases*. Report 404611-1, Texas Transportation Institute, College Station, TX.

Webster, S. L. (1979a). *Investigation of Beach Sand Trafficability Enhancement Using Sand-Grid Confinement and Membrane Reinforcement Concepts: Report 1, Sand Test Sections 1 and 2*. Technical Report GL-79-20, Geotechnical Laboratory, US Army Corps of Engineers Waterways Experimentation Station, Vicksburg, MS.

Webster, S. L. (1979b). *Investigation of Beach Sand Trafficability Enhancement Using Sand-Grid Confinement and Membrane Reinforcement Concepts: Report 2, Sand Test Sections 3 and 4*. Technical Report GL-79-20, Geotechnical Laboratory, US Army Corps of Engineers Waterways Experimentation Station, Vicksburg, MS.

Yang, X. and Han, J. (2013). "Analytical model for resilient modulus and permanent deformation of geosynthetic-reinforced unbound granular material." *ASCE Journal of Geotechnical and Geoenvironmental Engineering*, 139(9), 1443-1453.

Yang, X. Han, J., Leshchinsky, D., and Parsons, R. L. (2013). "A three-dimensional mechanistic-empirical model for geocell-reinforced unpaved roads." *Acta Geotechnica*, 8(2), 201-213.

Zhang, X. and Presler, W. (2012). *Use of H2Ri Wicking Fabric to Prevent Frost Boils in the Dalton Highway Beaver Slide Area, Alaska*. Alaska University Transportation Center. Fairbanks, AK.

Zornberg, J. G., Prozzi, J., Gupta, R., Luo, R., McCartney, J. S., Ferreira, J. Z., and Nogueira, C. (2008).

Validating Mechanisms in Geosynthetic Reinforced Pavements. TxDOT Research Report FHWA/TX-08/0-4829-1, The University of Texas at Austin, Austin, TX.